Analytically Integrated Results for Heavy Fermion Production in Two-Photon Collisions and a High Precision α_s Determination

B. Kamal

Physics Department, Brookhaven National Laboratory,

Upton, New York 11973, U.S.A.

Z. Merebashvili

High Energy Physics Institute,

Tbilisi State University, University st. 9, 380086 Tbilisi, Republic of Georgia.

Abstract

The cross section for massive fermion production in two-photon collisions was examined at next-to-leading order in QCD/QED for general photon helicity. The delta function (virtual+soft) part of the differential cross section was analytically integrated over the final state phase space. Series expansions for the complete differential and total cross sections were given up to tenth order in the parameter β. These were shown to be of practical use and revealed much structure. Accurate parametrizations of the total cross sections were given, valid up to higher energies. The above results were applied to top quark production in the region not too far above threshold. The cross section was shown to be quite sensitive to α_s in the appropriate energy region.

1 Introduction

High energy photons may be produced by backscattering laser light off high energy e^- or e^+ beams. In addition, high degrees of polarization are possible and the photons may carry a large fraction of the electron energy. Photon-photon collisions also arise naturally as a background in e^+e^- collisions. One major motivation for constructing a $\gamma\gamma$ interaction region at a high energy next linear collider (NLC) is to produce Higgs bosons on resonance via $\gamma\gamma$ fusion, which also allows direct determination of the $H\gamma\gamma$ coupling, which is sensitive to possible non Standard Model charged particles of large mass that may enter in the triangle loop. Using polarized photons allows one to control the backgrounds arising from $\gamma\gamma \to b\bar{b}$, for an intermediate mass Higgs [1]. This background has now been studied including QCD [2, 3, 4, 5] and electroweak [6] corrections.

In this talk we will consider in some detail the process $\gamma\gamma \to f\bar{f} + X$ in the region not too far above threshold, making use of the complete analytical results presented in [2], which include photon polarization. We will demonstrate the usefulness of $\gamma\gamma \to t\bar{t} + X$ in determining α_s precisely. We extend the analytical results presented in [2] by integrating and obtaining analytical results for the single integral (virtual+soft) part and by series expanding the entire differential and integrated cross section to order β^{10}, where β is the massive fermion velocity in the soft radiation limit. Such an expansion is shown to be of practical use, not too far above threshold, and it demonstrates many interesting features of the corrected cross sections. We have also provided parametrizations of the total integrated cross sections valid up to higher energies.

2 General form and decomposition of the differential cross section

The process under consideration is

$$\gamma(p_1, \lambda_1) + \gamma(p_2, \lambda_2) \to f(p_3) + \bar{f}(p_4) + [V(k)], \tag{1}$$

where λ_1, λ_2 denote helicities and the p_i, k denote momenta. f $(= q, l)$ represents a fermion with mass m and $V = g, \gamma$. The square brackets represent the fact that there may or may not be a gluon/photon in the final state. We have the following invariants,

$$s \equiv (p_1+p_2)^2, \quad t \equiv T-m^2 \equiv (p_1-p_3)^2-m^2, \quad u \equiv U-m^2 \equiv (p_2-p_3)^2-m^2 \tag{2}$$

and

$$s_2 \equiv S_2 - m^2 \equiv (p_1 + p_2 - p_3)^2 - m^2 = s + t + u. \tag{3}$$

Defining

$$v \equiv 1 + \frac{t}{s}, \qquad w \equiv \frac{-u}{s+t}, \qquad \beta \equiv \sqrt{1 - 4m^2/s}, \qquad x \equiv \frac{1-\beta}{1+\beta}, \tag{4}$$

we may express

$$t = -s(1-v), \qquad u = -svw, \qquad s_2 = sv(1-w), \qquad m^2 = \frac{s}{4}(1-\beta^2). \tag{5}$$

Now introduce

$$\kappa(s) \equiv 2\pi \frac{\alpha^2 e_f^4 [N_c]}{s}, \quad C_1 \equiv [C_F] \frac{\alpha_V}{2\pi}, \tag{6}$$

where the N_c, C_F factors are present only for f = quark and V = gluon, respectively and e_f is the fermion's fractional charge. Here

$$\alpha_V = \left\{ \begin{array}{ll} \alpha_s, & V = g \\ \alpha, & V = \gamma \end{array} \right. . \tag{7}$$

Then

$$\frac{d\sigma}{dvdw} = \frac{d\sigma^{(0)}}{dvdw} + \frac{d\sigma^{(1)}}{dvdw} \tag{8}$$

$$\equiv \kappa(s) \left[\frac{1}{2\pi} \frac{df^{(0)}}{dvdw} + \frac{C_1}{\pi} \frac{df^{(1)}}{dvdw} \right]. \tag{9}$$

The f functions are dimensionless functions of v and w, which allow us to parametrize our cross sections in an exact fashion, without dependence on α_V. We use the normalization convention of [7]. Since, in that normalization, the $f^{(i)}$ contain an overall factor of π, we consistently present analytical results for $f^{(i)}/\pi$ in order to cancel it. The unpolarized and polarized $f^{(i)}$ are given by

$$\begin{aligned} f^{(i)}_{\text{unp}} &= \frac{1}{2}[f^{(i)}(+,+) + f^{(i)}(+,-)], \\ f^{(i)}_{\text{pol}} &= \frac{1}{2}[f^{(i)}(+,+) - f^{(i)}(+,-)], \end{aligned} \tag{10}$$

in the notation $f^{(i)}(\lambda_1, \lambda_2)$. Define

$$j \equiv 1 - <\lambda_1 \lambda_2>, \tag{11}$$

where $<\lambda_1\lambda_2>$ is the average value of $\lambda_1\lambda_2$. Then

$$\begin{aligned} f^{(i)}(j) &= \frac{1+<\lambda_1\lambda_2>}{2} f^{(i)}(+,+) + \frac{1-<\lambda_1\lambda_2>}{2} f^{(i)}(+,-) \\ &= f^{(i)}(+,+) + \frac{j}{2}[f^{(i)}(+,-) - f^{(i)}(+,+)] = f^{(i)}(+,+) - j f^{(i)}_{\rm pol}, \end{aligned}$$

so that

$$j = \begin{cases} 0 & \rightarrow \quad f^{(i)}(j) = f^{(i)}(+,+) = f^{(i)}(-,-) \\ 2 & \rightarrow \quad f^{(i)}(j) = f^{(i)}(+,-) = f^{(i)}(-,+) \\ 1 & \rightarrow \quad f^{(i)}(j) = f^{(i)}_{\rm unp} \end{cases} . \tag{12}$$

The LO term is given by

$$\begin{aligned} &\frac{1}{2\pi}\frac{df^{(0)}(j)}{dvdw} = \\ &= \delta(1-w)\left\{\frac{2m^2/s}{v^2(1-v)^2}(1-2m^2/s) + j\left(\frac{1}{v(1-v)} - 2\right)\left[1 - \frac{2m^2}{sv(1-v)}\right]\right\} \\ &= \delta(1-w)\left\{\frac{1-\beta^4}{4v^2(1-v)^2} + j\left(\frac{1}{v(1-v)} - 2\right)\left[1 - \frac{1-\beta^2}{2v(1-v)}\right]\right\}. \end{aligned} \tag{13}$$

The last form shows explicitly the polynomial structure of the leading order differential cross section in terms of β. This is somewhat misleading, however, as we shall see in the next section, since the phase space in v itself depends on β.

From [2] we see that $df^{(1)}/dvdw$ has the form

$$\begin{aligned} \frac{1}{\pi}\frac{df^{(1)}}{dvdw} &= F_h(v,w) + \frac{F_s(v,w)}{(1-w)_+} + F_\delta(v)\delta(1-w) \\ &= F_h(v,w) + \frac{F_s(v,w) - F_s(v,1)}{1-w} + \\ &\quad + F_s(v,1)\ln(1-w_1)\delta(1-w) + F_\delta(v)\delta(1-w), \end{aligned} \tag{14}$$

where

$$w_1 = \frac{1-\beta^2}{4v(1-v)} \tag{15}$$

We have integrated analytically the terms proportional to the delta function part in the above equation. The terms F_i can be directly inferred from the expressions given in [2].

It is standard [8] to divide the cross section (i.e. $f^{(1)}$) into two parts. Firstly, there is the virtual plus soft part,

$$\frac{df^{(1)}_{\mathrm{V+S}}}{dvdw} = \frac{df^{(1)}_{\mathrm{V}}}{dvdw} + \frac{df^{(1)}_{\mathrm{S}}}{dvdw}, \tag{16}$$

where $df^{(1)}_{\mathrm{V}}/dvdw$ denotes the virtual contribution and $df^{(1)}_{\mathrm{S}}/dvdw$ is obtained by integrating the bremsstrahlung contribution to $df^{(1)}/dvdw$ over the region

$$1 \geq w \geq w_{1,\mathrm{soft}} \equiv 1 - \frac{m^2\delta}{sv}, \tag{17}$$

then multiplying by $\delta(1-w)$. We follow the definition of the soft parameter, δ, given in [8] such that the gluon/photon radiated becomes arbitrarily soft by making δ arbitrarily small. Since this takes into account all virtual corrections and soft radiation, the hard radiation may be taken into account by integrating $df^{(1)}/dvdw$ in the region $w_1 \leq w \leq w_{1,\mathrm{soft}}$. Since we never reach $w=1$, $F_s(v,w)/(1-w)_+ = F_s(v,w)/(1-w)$ in the hard radiation integration. We thus define $df^{(1)}_{\mathrm{H}}/dvdw$ as being $df^{(1)}/dvdw$ in the region $w_1 \leq w \leq w_{1,\mathrm{soft}}$, where the $\delta(1-w)$ terms do not contribute:

$$\frac{df^{(1)}_{\mathrm{H}}}{dvdw} = \frac{df^{(1)}}{dvdw}(w_1 \leq w \leq w_{1,\mathrm{soft}}). \tag{18}$$

The sum of the (integrated over some region) hard and soft contributions so defined is independent of δ in the limit $\delta \to 0$ and this method of separation is referred to as the *phase space slicing method*. As one might expect, there is a close relation between $df^{(1)}_{\mathrm{V+S}}/dvdw$ and $(df^{(1)}/dvdw)_\delta$ as well as between $df^{(1)}_{\mathrm{H}}/dvdw$ and $(df^{(1)}/dvdw)_{N\delta}$. Here subscript δ denotes terms in (14) multiplied by $\delta(1-w)$ and $N\delta$ the opposite. We give explicitly the necessary conversion terms in [9].

The variables v, w are suitable for performing analytical integration of the cross section (at least for the single integral part). They are not, on the other hand, suitable for performing series expansions of the integrated cross section about $\beta = 0$. The reason is that, in these variables, the integration limits depend on β so that the series expansion of the integrated cross section does not follow straightforwardly from the series expansion of the differential cross section, and we only have complete analytical results for the differential cross sections. Otherwise, we could just expand the final integrated result. The above will become clear in the following.

At this point, we introduce a new set of variables, τ and ω, suitable for performing series expansions in β. They are defined through

$$v \equiv \frac{1}{2}(1+\tau\beta), \qquad w \equiv 1 - c_\beta(\tau)\beta^2(1-\omega), \tag{19}$$

where

$$c_\beta(\tau) \equiv \frac{1-\tau^2}{1-\tau^2\beta^2}. \tag{20}$$

We note

$$\frac{df^{(i)}}{d\tau d\omega} = \frac{\beta^3 c_\beta(\tau)}{2}\frac{df^{(i)}}{dvdw}. \tag{21}$$

Because of the factor $c_\beta(\tau)$, $df^{(i)}/d\tau d\omega$ will never get a part proportional to $\delta(1\pm\tau)$. Defining

$$c_u \equiv c_\beta(\tau)(1-\omega)(1+\tau\beta), \tag{22}$$

the invariants are given by

$$\begin{aligned}
t &= -\frac{s}{2}(1-\tau\beta), \qquad u = -\frac{s}{2}(1+\tau\beta-\beta^2 c_u), \qquad s_2 = \frac{s}{2}c_u\beta^2, \\
T &= -\frac{s}{4}(1-2\tau\beta+\beta^2), \\
U &= -\frac{s}{4}[1+2\tau\beta+\beta^2(1-2c_u)], \qquad S_2 = \frac{s}{4}[1+\beta^2(2c_u-1)].
\end{aligned} \tag{23}$$

In terms of τ and ω, the LO term has the form

$$\frac{1}{2\pi}\frac{df^{(0)}(j)}{d\tau d\omega} = \frac{\beta\delta(1-\omega)}{(1-\tau^2\beta^2)^2}[2(1-\beta^4) - j(1+\tau^2\beta^2)(1+\tau^2\beta^2-2\beta^2)] \tag{24}$$

$$= \delta(1-\omega)[(2-j)\beta + (2j+4\tau^2-4j\tau^2)\beta^3 + \mathcal{O}(\beta^5)]. \tag{25}$$

We see explicitly that the $j=0,1$ differential cross sections, in terms of these variables, vanish by order β in the limit $\beta \to 0$, while the $j=2$ differential cross section is order β^3.

3 Analytic integration of the delta function part

The only complete analytical results for the differential cross sections were presented in [2]. Analytical results for the virtual+soft part were presented in [8] for the unpolarized case and in [3] for the polarized case (where the virtual and soft parts are given separately, in terms of various functions). Still, not even the virtual+soft part has previously been integrated (over fermion angle) analytically. In this section, we present such an analytical integration. We were not able to integrate the non delta function (or hard) part analytically, in a straightforward fashion, and reserve that for future work.

The integrated cross section (or $f^{(i)}$) is obtained via

$$f^{(i)} = \int_{v_1}^{v_2} dv \int_{w_1}^{1} dw \frac{df^{(i)}}{dv dw} = \int_{-1}^{1} d\tau \int_{0}^{1} d\omega \frac{df^{(i)}}{d\tau d\omega} , \tag{26}$$

where

$$v_1 = \frac{1}{2}(1-\beta), \qquad v_2 = \frac{1}{2}(1+\beta). \tag{27}$$

Let θ_3 be the angle between p_3 and p_1 in the $\gamma\gamma$ c.m. Then θ_3 is given by

$$\cos\theta_3 = -\frac{1-v-vw}{\sqrt{(1-v+vw)^2+\beta^2-1}} \tag{28}$$

$$= \frac{2\tau-\beta c_u}{\sqrt{4-c_u(4-\beta^2 c_u)}} . \tag{29}$$

Thus,

$$\cos\theta_3 = -\frac{1-2v}{\beta} = \tau, \qquad \text{for } w=\omega=1. \tag{30}$$

We see that for $\beta \to 0$, $\cos\theta_3$ varies rapidly with v, while it is simply equal to τ. This is why the phase space in v becomes vanishingly small by order β. Similarly, from (26) and (15), or (19), we see that the w phase space is order β^2. Thus, the double integration over v and w is order β^3, in accord with (21).

The integration of (13) or (24) is rather straightforward, yielding the LO term,

$$\frac{f^{(0)}(j)}{2\pi} = 2\beta(1+\beta^2) - 6\beta j - (1-\beta^4+2j)\ln x. \tag{31}$$

Since

$$\ln x = -2\sum_{k=0}^{\infty}\frac{\beta^{2k+1}}{2k+1} = -2\beta - 2\frac{\beta^3}{3} - \cdots, \tag{32}$$

we have

$$\frac{f^{(0)}(j)}{2\pi} = 2(2-j)\beta + \frac{4(2+j)}{3}\beta^3 + 2\sum_{k=2}^{\infty}\left(\frac{-1}{2k-3} + \frac{1+2j}{2k+1}\right)\beta^{2k+1}, \tag{33}$$

so that $f^{(0)}(0,1)$ are order β and $f^{(0)}(2)$ is order β^3. Also, we see that only $f^{(0)}(0)$ is finite in the limit $\beta \to 1$ and it approaches

$$f^{(0)}(0) \to 8\pi, \qquad \text{for } \beta \to 1\ . \tag{34}$$

We denote the single and double integral contributions to $f^{(1)}$ by

$$f^{(1)}_{si/di} \equiv \int_{v_1}^{v_2} dv \int_{w_1}^{1} dw \left(\frac{df^{(1)}}{dvdw}\right)_{\delta/N\delta} \tag{35}$$

$$= \int_{-1}^{1} d\tau \int_{0}^{1} d\omega \left(\frac{df^{(1)}}{d\tau d\omega}\right)_{\delta/N\delta}. \tag{36}$$

We performed the single integration using (35), as opposed to (36). It turned out to be quite lengthy and involved. Our final (simplified) result is

$$\begin{aligned}
\frac{f^1_{si}}{\pi} &= a_1\pi^2/6 + a_2\mathrm{Li}_2(x) + a_3\mathrm{Li}_2(-x) + \frac{\ln(x)}{\beta}[a_4\mathrm{Li}_2(x) + a_5\mathrm{Li}_2(-x)] \\
&+ a_6\ln[(1+\beta)/2][\pi^2/6 + 2\mathrm{Li}_2(-x)] \\
&+ a_7\ln(x)\pi^2/6 + a_8\{-3\ln^2[(3+\beta^2)/4]\ln(x) \\
&+ 5\ln[(1-\beta^2)/4]\ln[(3+\beta^2)/4]\ln(x) + 2\mathrm{Li}_3[-2x/(1+\beta)] \\
&- 2\mathrm{Li}_3[-2/(x(1-\beta))] + 2\mathrm{Li}_2[(1-\beta)^2/(3+\beta^2)]\ln[2/(x(1-\beta))] \\
&- 2\mathrm{Li}_2[(1+\beta)^2/(3+\beta^2)]\ln[2x/(1+\beta)]\} \\
&+ a_9\{\mathrm{Li}_3[(1+\beta)/2] - \mathrm{Li}_3[(1-\beta)/2]\} \\
&+ a_{10}\ln(x) + a_{11}\ln^3(x)/\beta + a_{12}\ln^2(x)/\beta + a_{13}\ln^2[(1+\beta)/2]\ln(x) \\
&+ a_{14}\beta + [a_{15} + a_{16}\ln^2(x)/\beta^2]\beta\ln(\beta) \\
&+ [a_{17}\beta + a_{18}\ln(x) + a_{19}\ln^2(x)/\beta]\ln[(1+\beta)/2].
\end{aligned} \tag{37}$$

The coefficients $a_i(j)$ are given in [9] and are rational polynomials in β, finite as $\beta \to 0$. Terms of the form $F(\beta) - F(-\beta)$ will vanish for $\beta = 0$. Noting that

$$\mathrm{Li}_2(1) = \frac{\pi^2}{6}, \qquad \mathrm{Li}_2(-1) = -\frac{\pi^2}{12}, \tag{38}$$

we see that only the terms proportional to $a_1, \ldots, a_5$ may contribute at threshold, which is the case for $j = 0$. Indeed, one finds the correct threshold correction from those terms alone. The relevant series expansions will be given in the next section. As we shall see in Section V, the double integral series expansion starts at order β^3.

Two independent determinations of (37) were made using Mathematica [10] and REDUCE [11]. That software could not evaluate certain integrals which can be found in [12]. It was verified that the analytically integrated result agreed numerically with the numerically integrated result. In the next section, we will show how one can use the series expansion as a very solid check as well.

Perhaps the most convincing check of (37) and the analytical result for $df^{(1)}/dvdw$ (or $d\sigma_{\mathrm{NLO}}/dvdw$) obtained in [2] is the excellent numerical agreement with tabulated results for $f^{(1)}$ existing in the literature. The only existing analytical results, aside from those in [2], are the expressions for $df^{(1)}_{\mathrm{V+S}}/dvdw$ (i.e. $(df^{(1)}/dvdw)_\delta$), $df^{(1)}_{\mathrm{S}}/dvdw$ given in [8] for the unpolarized case (using dimensional regularization), with which we agree exactly, and similar expressions for the polarized case in [3] (obtained using a gluon energy cut and a small gluon mass as infrared regulator). The latter are not quite in a form suitable for direct analytical comparison. There have been no other analytical results presented for $(df^{(1)}/dvdw)_{N\delta}$ in the polarized or unpolarized cases. Hence we must perform the above mentioned numerical checks.

Define

$$z \equiv \frac{\sqrt{s}}{2m} = \frac{1}{\sqrt{1-\beta^2}} \longleftrightarrow \beta = \sqrt{1 - 1/z^2}\ . \tag{39}$$

In Table 1 we give numerically computed values for $f^{(1)}_{\mathrm{unp}}$, $f^{(1)}_{\mathrm{pol}}$, $f^{(1)}(+,+)$, $f^{(1)}(+,-)$ as well as the specific contributions from all the $f^{(1)}_{si}$ and $f^{(1)}_{di}$ to the corresponding $f^{(1)}$, for various values of $1.2 \le z \le 20$. The result at $z = 1$ is given exactly by the series expansions presented in the next section.

We also indicate the number of significant figures, n.s., following the decimal point, in $f_{di}^{(1)}$ (and $f^{(1)}$).

The next issue is, of course, how well these values compare with other tabulated values for $f^{(1)}$. Two other such tables exist at present. The original one of [7] gave $f_{\rm unp}^{(1)}$ for $z = 2, 3, 4, 5, 10$; the value at $z = 1$ being numerically equal to the known threshold result, as given in the next section. Their numerical values were obtained using the $f_{\rm V+S}^{(1),\rm unp}$ given in [8], added numerically to $f_{\rm H,unp}^{(1)}$, determined there using the same methodology as [8], which is equivalent to our method. We find numerical agreement with [7] to within the precision of those values, which is roughly at the order of one part in $10,000$ or better. This can only be achieved with correct analytical results. Our calculation of $f_{\rm pol}^{(1)}$ is identical in method (same integrals and structure) to that of $f_{\rm unp}^{(1)}$ (at the differential and integrated level), the only difference arising from different traces due to the contraction with a polarized photonic tensor rather than an unpolarized one. As two independent determinations of these traces were performed, there is little room for any error in $f_{\rm pol}^{(1)}$. Fortunately, we may directly check this assertion since the values of $f^{(1)}(+,+)$ and $f^{(1)}(+,-)$ for $z = 2, 3, 4, 5, 10, 20, 50$ were tabulated in [3]. There, Monte Carlo methods were used, leading to accuracy at the level of better than 1% in regions where the $f^{(1)}$ are sizable, but apparently not better than ± 0.2 or so in absolute error. This absolute error is noticeable only for $f^{(1)}(+,+)$ and only for $z = 2, 3$, where $f^{(1)}(+,+)$ is small. To within the above accuracy, we are in good agreement with [3]. Since $f^{(1)}(+,-) = f_{\rm unp}^{(1)} - f_{\rm pol}^{(1)}$ and since we have precision agreement with [7] for $f_{\rm unp}^{(1)}$ and with [3] for $f^{(1)}(+,-)$, we conclude that our analytical results for $df_{\rm pol}^{(1)}/dvdw$ of [2] have been verified. In light of the above, Table 1 is seen to be the most complete and precise such table at present.

4 Series expansion of the delta function part

Besides providing a useful check of the analytical integration of the previous section, there are many reasons why it is useful and instructive to series expand the differential and integrated cross sections about $\beta = 0$. In the absence of complete analytically integrated results, only a series expansion about $\beta = 0$ can be used to make (very) high precision predictions in the $\beta \simeq$

0 region. One also sees the structure of the cross section in a way that cannot be inferred from the non-expanded analytical results, which are somewhat complicated. From a practical viewpoint, having "simple" series expansions for the differential cross sections allows one to do complete numerical studies in the region not too far above threshold rather easily. This is because the resulting expansions only involve simple polynomials and simple logarithms. We will address the issue of the region of validity of the expansions as well.

The other issue is that of resummation. There are large correction terms at threshold which can be resummed. Having a series expansion of high enough order to be of practical use allows one to explicitly perform resummations up to some order in β while leaving the higher order terms the same. The net result would be an equally simple series, improved via resummation so as to allow one to go closer to threshold. This is beyond the scope of this paper as are other very near threshold effects. Suffice it to say that having the threshold series expansion will facilitate these studies for those interested.

Throughout, we will expand up to order β^{10} (including $\beta^{11}\ln\beta$ terms). The expansion which exists in the literature (see [7]) is only for $f^{(1)}_{\rm unp}$ and only goes to order β. Going to order β^{10} may seem excessive at first, but we found it to be a good stopping point for several reasons. Considerable structure arises beyond order β which allows us to see the general, all-orders in β, structure of the various series. Also, one gains little in terms of precision by going to even higher orders in β, without including several more terms.

We find that $d\tilde{f}^{(1)}/d\tau d\omega$ may be expanded in the general form

$$\frac{d\tilde{f}^{(1)}}{d\tau d\omega} = \sum_{i=0}^{\infty}\sum_{j=0}^{1} c_{ij}(\tau,\omega)\beta^i \ln^j\beta. \tag{40}$$

Therefore $f^{(1)}$ may be expanded as

$$f^{(1)} = \tilde{f}^{(1)} = \sum_{i=0}^{\infty}\sum_{j=0}^{1} d_{ij}\beta^i \ln^j\beta, \tag{41}$$

where the d_{ij} are given by

$$d_{ij} = \int_{-1}^{1} d\tau \int_{0}^{1} d\omega\, c_{ij}(\tau,\omega). \tag{42}$$

With the variables v and w, the integration limits depend on β, hence the above arguments do not hold. So, one sees clearly the necessity of the change of variables.

We convert from $(df^{(1)}/dvdw)_\delta$ to $(df^{(1)}/d\tau d\omega)_\delta$ using (21), which modifies the overall factor via $\delta(1-w) \to \beta^3 c_\beta(\tau)\delta(1-w)/2 = \beta\delta(1-\omega)/2$. The compact results for the series expansions of $(df^{(1)}/d\tau d\omega)_\delta$ for $j=0$ and $j=2$ can be found in [9], up to order β^{10}.

The expansions have rather simple structure in that the $c_{ij}(\tau)$ are simply polynomials in τ. This amounts to considerable simplification and reduction in computational time relative to the exact expressions, especially after the non delta function part is added, where the simplification is even greater as we shall see in the next section.

Assuming we are working at β where the series are sufficiently accurate, one could easily analytically integrate them over a region of τ ($\cos\theta_3$) relevant to some experiment, if desired, and implement angular cuts analytically. After a suitable change of variables, the same could be done for the hard radiation part, either analytically or numerically. Cuts on additional observables may be made by subtracting off the unwanted configurations using the squared amplitudes given in [2] and Monte Carlo integration, for instance. Here, we simply present the total integrated results.

For the $j=0$ channel, we find

$$
\begin{aligned}
&\frac{1}{\pi} f_{si}^{(1)}(+,+) = \qquad (43)\\
&\quad 2\Big\{2\pi^2 - (20-\pi^2)\beta + 10/3\pi^2\beta^2 + \beta^3/3[-340/3 + \pi^2 + 64\ln(2\beta)]\\
&\quad +8/15\pi^2\beta^4 + 4/15\beta^5[-6343/45 - \pi^2 - 32\ln(2) + 256/3\ln(2\beta)]\\
&\quad -104/105\pi^2\beta^6 + 4/105\beta^7[-39163/315 - \pi^2 + 208/3\ln(2\beta)]\\
&\quad -88/315\pi^2\beta^8 + 4/9\beta^9\{1/7[-\pi^2/5 - 64/3\ln(2)]\\
&\quad +1/25[128\ln(2\beta) - 43903/315]\} - 488/3465\pi^2\beta^{10}\\
&\quad +103232/51975\beta^{11}\ln(2\beta)\Big\}
\end{aligned}
$$

and for $j=2$,

$$
\begin{aligned}
&\frac{1}{\pi} f_{si}^{(1)}(+,-) = \qquad (44)\\
&\quad 16/3\Big\{\pi^2\beta^2 - 8\beta^3 + \pi^2\beta^4 + 32\beta^5[-289/720 + \ln(2)/5 + \ln(2\beta)/3]
\end{aligned}
$$

$$+\pi^2/7\beta^6 + 6/5\beta^7[-3947/945 + 16/7\ln(2) + 32/9\ln(2\beta)] + 29/105\pi^2\beta^8$$
$$+4/15\beta^9[-823/45 + 8\ln(2) + 16\ln(2\beta)] + 289/1155\pi^2\beta^{10}$$
$$+256/63\beta^{11}\ln(2\beta)\Big\}.$$

The results are indeed quite simple. We may again obtain $\frac{1}{\pi}f^{(1)}_{\mathrm{V+S}}$ by adding the corresponding conversion term [9].

The strongest check comes from the fact that the expansions (43), (44) which come from integrating (40), (41) agree exactly with the expression obtained by expanding the analytically integrated result (37) directly. In this way, we simultaneously check all the above mentioned expressions, including our analytical integration (37). The expansions (43), (44) were also checked numerically by subtracting them from the exact expression (37) and verifying that the difference was order β^{11}.

5 Series expansion of the non delta function part

Perhaps the most remarkable result of the series expansion is the simplification of the non delta function part, whose original form is the most lengthy part of the exact result, involving complicated logarithms, etc... Although the intermediate expressions were very lengthy and considerable computational time was required, a large degree of cancellation resulted in the following simple series. We convert from $(df^{(1)}/dvdw)_{N\delta}$ to $(df^{(1)}/d\tau d\omega)_{N\delta}$ by multiplying by $\beta^3 c_\beta(\tau)/2$. Again, we present here results for the total cross sections, the results for the differential cross sections can be found in [9]. The integration of differential cross sections over τ, ω is straightforward and we obtain

$$\frac{1}{\pi}f^{(1)}_{di}(+,+) = \frac{-128}{9}\beta^3 - \frac{448}{225}\beta^5 + \frac{34624}{2205}\beta^7 + \frac{42368}{3675}\beta^9, \tag{45}$$

$$\frac{1}{\pi}f^{(1)}_{di}(+,-) = \frac{-1024}{45}\beta^5 - \frac{2816}{525}\beta^7 - \frac{134656}{19845}\beta^9. \tag{46}$$

We notice the absence of any logarithms, including powers of $\ln\beta$. The structure is fairly predictable as well. We see that the series begin at order β^3 and β^5 for $j=0$ and $j=2$ respectively, so that their effect will be negligible very near to threshold. On the other hand, the large coefficients imply that they soon become noticeable for small β.

These are remarkably simple results, which suggest that the exact integrated result for $f_{di}^{(1)}$ is not too complicated. We notice the vanishing of the coefficients of the even powers of β. This follows from the antisymmetry in τ of the corresponding terms in the differential cross section. For discussion about the conversion terms see [9].

6 Total series result and numerical parametrizations

We are now in a position to study the total cross section, by combining the results of the previous sections. Adding (43) and (45) gives the series for the $j = 0$ total cross section and adding (44), (46) gives the series for the $j = 2$ total cross section.

In Table 2 we present the fractional error on the series for $f^{(1)}(+,+)$, $f^{(1)}(+,-)$, $f_{\mathrm{unp}}^{(1)}$ relative to the result obtained using numerical integration, for various values of z in the region $1.05 \leq z \leq 1.4$. For $z \lesssim 1.05$, the series expansions are more accurate than the numerical results. At $z = 1.05$, the errors are at the 10^{-7}–10^{-6} level. For $z = 1.2$ they are at the 10^{-4}–10^{-3} level and for $z = 1.4$ they are at the $10^{-3} - 10^{-2}$ level. The errors on $f^{(1)}(+,+)$ are at the lower end, while the errors on $f^{(1)}(+,-)$ are at the higher end and those for $f_{\mathrm{unp}}^{(1)}$ lie in between. This is good because, as we shall see in the next section, in determining α_s via top quark production at a $\gamma\gamma$ collider, it is the $j = 0$ and unpolarized channels which are of interest, the $j = 0$ channel being the most interesting one. With precision of better than one percent for $z \leq 1.4$, we have sufficient accuracy to use the series expansions (differential in particular) to perform easy numerical studies relevant to top quark production at a $\gamma\gamma$ collider of $\sqrt{s} \lesssim 500$ GeV. As we shall see, for the α_s determination, going to much higher energies is not useful since the determination is best done near $z = 1.2$ ($\sqrt{s} \simeq 420$ GeV).

It is also useful to be able to parametrize $f^{(1)}$ to good accuracy for larger β, relevant for bottom and charm quark production at intermediate energies or top quark production at very high energies. This was done by fitting numerically computed values of $f^{(1)}$. We divide the parametrizations into 3 regions: a low energy region ($1 \leq z \leq 1.5$ or $0 \leq \beta \leq 0.7454$), an intermediate energy region ($1.5 < z \leq 5$) and a high energy region ($5 < z \leq 20$).

The various forms for the parametrizations are are given in [9]. In the low energy region, where high accuracy is required, the parametrizations are accurate to $\lesssim 0.01\%$, with the errors being the largest near the higher end of the region. The leading terms, given analytically, guarantee the correct threshold behaviour as they are just those in the exact series expansion. As mentioned earlier in connection with the series expansions, one can explicitly perform resummations on those terms. Thus one could modify the above parametrizations to include resummation effects without changing the higher order coefficients.

7 Precision α_s determination from top-quark production

A high energy $\gamma\gamma$ collider can be used as a "factory" for many interesting particles: Higgs bosons, $W^{\pm}$ bosons, top quarks etc... The beam polarization we be useful in producing Higgs bosons and reducing $Q\overline{Q}$ backgrounds. More specifically, the $j = 0$ channel will be of interest. This channel also turns out to be the channel of interest when trying to determine α_s via top quark production, making it complementary to the Higgs studies. The reason is that the cross section, and QCD corrections, are enhanced in this channel, thereby improving the statistics and the determination of α_s, to which the cross section will be quite sensitive. The process $\gamma\gamma \to t\bar{t}+X$ is more powerful than $e^+e^- \to Q\overline{Q} + X$ in determining α_s because the QCD corrections are quite small in the latter, thus requiring an unreasonably large number of events for high precision; the corrections are suppressed by $\alpha_s/\pi \simeq 4\%$, relative to the Born term. In $\gamma\gamma \to t\bar{t}+X$, we can "pick" our QCD correction by choosing the appropriate beam energy. Of course, as one gets too close to threshold, the perturbation series cannot be trusted. Hence there are limitations.

To best illustrate the above idea, in Fig. 1 we have plotted the $\gamma\gamma \to t\bar{t}+X$ cross section at LO and NLO, in the region $1 \leq z \leq 1.4$, for the various helicity states. We took $N_f = 5$, $m_t = 174$ GeV and used $\Lambda = 230$ MeV in the two-loop expression for α_s, evaluated at $\mu^2 = s$. One could also use

$N_f = 6$, but since we are not far above threshold it is simpler to use $N_f = 5$ for evolution from $\mu^2 = M_Z^2$ to $\mu^2 = s$. We notice that the $j = 0$ cross section is the largest, as are its QCD corrections, in this region. The region $z \simeq 1.2$ is nice in that the $j = 0$ cross section is near its maximum and the QCD corrections are sizable ($\simeq$ 20% of the total cross section), yet not so large that the perturbative expansion is unreliable. As one gets closer to threshold, other higher order effects, nonperturbative effects and top width effects may also become important. For these, and other reasons to be considered below, we will suggest $z = 1.2$ as being the optimal region for extracting α_s and we will give a rough estimate of how precisely α_s may be determined there. As well, we suggest the $j = 0$ channel as being the most powerful.

Firstly, we note that $z = 1.2$ corresponds to $\sqrt{s_{\gamma\gamma}} \simeq 420$ GeV, for top quark production. This energy should be accessible at a $\sqrt{s_{e^+e^-}} \gtrsim 500$ GeV NLC. A typical $\gamma\gamma$ luminosity assumed is 20 fb^{-1}. Since $\sigma \simeq 1.4$ pb, this corresponds to roughly 28,000 $t\bar{t}$ events. Since the QCD correction is $\sim 20\%$ of the total cross section, this translates to $\Delta\alpha_s/\alpha_s \simeq 3\%$, statistically. With a luminosity increase and, possibly, extended running, one could envision going to the percent level or better.

The above analysis was purely based on statistics and one-loop QCD corrections. Therefore, we will briefly discuss various theoretical systematic uncertainties. Clearly, one needs a two-loop analysis when dealing with one-loop corrections of order 20%, in order to determine α_s at the level of a few percent. Threshold resummation can also be performed. One should also take into account the one-loop electroweak corrections [6]. The QED ones are identical in form to the QCD ones, with the appropriate change in normalization, given by (6). There will be a minor dependence on m_t, which will be lessened with future Fermilab runs. The uncertainty on m_t translates to an uncertainty on z. Since the $j = 0$ cross section is near its peak for $z \simeq 1.2$, minor variations in z will not appreciably affect the results.

Of some concern are resolved photon contributions, where a gluon or quark within the photon can participate directly in the interaction. Suppression of these contributions is a major reason for working close to threshold. Since the parton distributions within the photon drop steeply with increasing momentum fraction, x, and since x must be large near threshold, such contributions are quite suppressed. Confirmation of this assertion may be inferred from the resolved contributions to b quark production near threshold presented in [13] from which we conclude that only very poor knowledge (if any) of the photon structure will be required, as such contributions will be a fraction of a percent of the cross section. One can further reduce those contributions by identifying outgoing jets collinear with one of the photon beams, which are a signature of resolved photon events. One can also require that the energy deposited in the detectors be equal to the total beam energy in order to account for missed jets of the type mentioned above.

From the experimental side, we are assuming only that $t\bar{t}$ events can be clearly identified. With experience gained from Fermilab, this seems reasonable, especially considering the cleaner initial and final states in the $\gamma\gamma$ case. Another experimental issue is that of normalization. We suggest the measurement of a ratio

$$R^{\gamma\gamma}_{Q/P} \equiv \frac{\sigma(\gamma\gamma \to Q\overline{Q} + X)}{\sigma(\gamma\gamma \to P\overline{P} + X)}, \qquad P = W, l. \tag{47}$$

The ratio of $t\bar{t}$ to W^+W^- events is statistically quite powerful as over one million W^+W^- events are expected at such a "W factory" [14]. This highlights the complementary nature of top quark and $W^\pm$ production at a $\gamma\gamma$ collider. As well, electroweak corrections to W^+W^- production have been studied [14].

It is worth discussing the many advantages of determining α_s via $\gamma\gamma \to t\bar{t}+X$ relative to some of the options currently being used. The calculation is perturbative and avoids nonperturbative contributions arising in α_s determinations from mass splittings and tau decays. Other determinations, based on evolution of hadronic structure functions, rely on the parton model and assumed knowledge of hadronic structure. No such assumptions are made here. Unlike the 3- to 2-jet ratio from e^+e^- annihilation, we avoid having to define the jet isolation criteria by measuring the total $t\bar{t}$ cross section. Since we are at a large energy scale, not only does perturbation theory work well, but we automatically determine α_s at (or above) the $t\bar{t}$ threshold, without having to perform evolution or cross flavor thresholds. From a theoretical viewpoint, the most comparably clean determination comes from the ratio of hadrons to lepton pairs produced in e^+e^- annihilation at the Z pole. As mentioned earlier, the small QCD correction proves an insurmountable limiting factor in that case.

References

[1] J.F. Gunion and H.E. Haber, Phys. Rev. D **48**, 5109 (1993).

[2] B. Kamal, Z. Merebashvili, and A.P. Contogouris, Phys. Rev. D **51**, 4808 (1995); D **55**, 3229(E) (1997).

[3] G. Jikia and A. Tkabladze, Phys. Rev. D **54**, 2030 (1996).

[4] D.L. Borden, V.A. Khoze, J. Ohnemus, and W.J. Stirling, Phys. Rev. D **50**, 4499 (1994).

[5] V.S. Fadin, V.A. Khoze, and A.D. Martin, Phys. Rev. D **56**, 484 (1997).

[6] A. Denner, S. Dittmaier, and M. Strobel, Phys. Rev. D **53**, 44 (1996).

[7] J.H. Kühn, E. Mirkes, and J. Steegborn, Z. Phys. C **57**, 615 (1993).

[8] W. Beenakker, H. Kuijf, W.L. van Neerven, and J. Smith, Phys. Rev. D **40**, 54 (1989).

[9] B. Kamal and Z. Merebashvili, Phys. Rev. D (in print), hep-ph/9803350.

[10] S. Wolfram, *Mathematica User's Manual*, Addison Wesley, 1991.

[11] A.C. Hearn, *REDUCE User's Manual Version 3.6* (Rand Corporation, Santa Monica, CA, 1995).

[12] L. Lewin, *Polylogarithms and Associated Functions*, North Holland, 1981.

[13] M. Drees, M. Krämer, J. Zunft, and P.M. Zerwas, Phys. Lett. **B306**, 371 (1993).

[14] G. Jikia, Nucl. Phys. **B494**, 19 (1997).

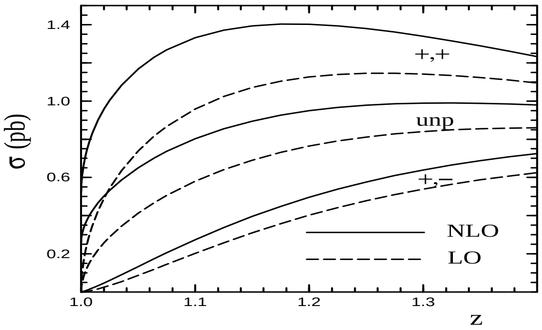

Figure 1: The $\gamma\gamma \to t\bar{t} + X$ cross section at LO and NLO, versus z, for the various helicity states.

Table 1: The various $f^{(1)}$ for values of $1.2 \leq z \leq 20$, and the corresponding single and double integral contributions. Here n.s. is the number of significant figures *after* the decimal point in $f^{(1)}$ and $f_{di}^{(1)}$.

		$f^{(1)}_{si,\mathrm{unp}}$	$f^{(1)}_{di,\mathrm{unp}}$	$f^{(1)}_{\mathrm{unp}}$	$f^{(1)}_{si,\mathrm{pol}}$	$f^{(1)}_{di,\mathrm{pol}}$	$f^{(1)}_{\mathrm{pol}}$
z	n.s.	$f_{si}^{(1)}(+,+)$	$f_{di}^{(1)}(+,+)$	$f^{(1)}(+,+)$	$f_{si}^{(1)}(+,-)$	$f_{di}^{(1)}(+,-)$	$f^{(1)}(+,-)$
1.2	4	70.578894	-5.47998017	65.0989	33.4162848	-1.37661828	32.0397
	4	103.9951788	-6.85659845	97.1386	37.1626092	-4.10336189	33.0592
2	3	68.5516	-24.064	44.488	-76.4447	38.792	-37.653
	3	-7.8931	14.728	6.835	144.9963	-62.856	82.140
3	3	92.2075	-29.594	62.614	-191.7554	125.8526	-65.903
	3	-99.5479	96.259	-3.289	283.9629	-155.447	128.516
4	3	132.0495	-33.0381	99.011	-285.7603	215.4483	-70.312
	3	-153.7108	182.4102	28.699	417.8098	-248.4864	169.323
5	3	176.7014	-36.802	139.899	-367.5540	299.902	-67.652
	3	-190.8526	263.100	72.247	544.2554	-336.704	207.551
10	3	395.3262	-55.3625	339.964	-688.1880	639.5445	-48.6435
	3	-292.8618	584.182	291.320	1083.5142	-694.907	388.607
20	1	749.8886	-79.437	670.45	-1140.3966	1086.967	-53.43
	1	-390.5080	1007.530	617.02	1890.2852	-1166.404	723.88

Table 2: The fractional errors on the various $f^{(1)}$ computed using the series expansions up to order β^{10}, for values of $1.05 \leq z \leq 1.4$.

z	β	f. err$(+,+)$	f. err$(+,-)$	f. err$_{\mathrm{unp}}$	β^{11}
1.05	.3049	2.1×10^{-7}	2.5×10^{-6}	4.3×10^{-7}	2.1×10^{-6}
1.1	.4166	-6.8×10^{-6}	2.3×10^{-4}	3.1×10^{-5}	6.6×10^{-5}
1.2	.5528	-2.0×10^{-4}	3.3×10^{-3}	6.9×10^{-4}	1.5×10^{-3}
1.3	.6390	-1.4×10^{-3}	1.3×10^{-2}	3.4×10^{-3}	7.3×10^{-3}
1.4	.6999	-5.6×10^{-3}	2.9×10^{-2}	8.9×10^{-3}	2.0×10^{-2}